Indonesian Journal of Electrical Engineering and Informatics (IJEEI)
Vol. 11, No. 1, March 2023, pp. 50~60
ISSN: 2089-3272, DOI: 10.52549/ijeei.v11i1.4224

PI-based ZSVM control of Quasi-Z-Source Inverter for Photovoltaic Applications in Standalone Mode

Essaid Jaoide[1], Faicel El Aamri [2], Mbarek Outazkrit[1], Abdelhadi Radouane [1], Azeddine Mouhsen[1]
[1]Laboratory of Radiation-Matter and Instrumentation, Faculty of Science and Technology, University Hassan 1st, Settat, Morocco
[2] Laboratory of Materials, Energy and System Control, Hassan II University, FST of Mohammadia, Morocco

Article Info

Article history:

Received Oct 13, 2022
Revised Jan 13, 2023
Accepted Feb 2, 2023

Keyword:

Quasi-Z-Source inverter
Small signal model
Shoot-through state
ZSVM control
Standalone mode

ABSTRACT

The power converters Z-source topology are becoming a promoter solution for the energy conversion. This topology has the ability to boost and convert the voltage in a single-stage, unlike the famous two-stage conventionnel structure. The Quasi-Z-Source Inverter (QZSI) is nowadays the subject of several research works. However, it is the most suitable for PV applications, due to his continuous input current, which allows to harvest the maximum power available from the PV panels. In this regard, this paper investigates the dynamic characteristics of the QZSI through the small signal analysis, as well as the scheme control with the SVPWM technique for QZSI in standalone mode. The simulation results illustrate the practicability and the validity of the control scheme proposed.

Corresponding Author:

Essaid JAOIDE
Laboratory of Radiation-Matter and Instrumentation,
Faculty of Science and Technology,
University Hassan 1st, Settat, Morocco
Email: e.jaoide@uhp.ac.ma

1. INTRODUCTION

Over the last two decades, energy production from renewable sources has become a strategic sector worldwide. Where, this sector has developed rapidly and its penetration level is still growing, motivated by the increasing demand of clean energy and the trend for countries to reduce the use of fossil fuels [1], [2].In particular, the development of renewable energy has been heavily dominated by solar PV. In fact, more than half of all new renewable energy installations in 2017 were for PV solar energy. This has prompted extensive research efforts over the last two decades. The rapid development of solar PV is accompanied by the development of power converters, so as to collect the maximum power from the PV system [1]–[3]. In this context, the topology of Z-source converters, recently proposed [4], is the subject of several research works. This topology has attracted the attention of researchers, it offers several advantages over the conventional two-stage conversion structure [1], [2], [4]. However, the two-stage conversion structure, as described in [1], [2], [5], suffers from higher cost and reduced efficiency due to the presence of two power stages in cascade.
In this context, the Z-source converter allows to increase the DC input voltage in a single-stage and converts it into AC voltage adapted to the load or the grid. Given that this family of converters uses two capacitors and two inductors in X-shape [2]–[4], [6].

The discontinuous input current of the Z-source converter makes its uses uneconomical for PV applications, where high gain and continuous input current are crucial [1]–[3]. As a solution, Figure 1 shows the quasi-Z-source inverter that inherits the same properties of ZSI without the discontinuous input current [7]. Consequently, it allows maximum power harvesting from the PV panels [1], [2]. Indeed, since it appeared,

Several research studies have investigated the feasibility of using QZSI for PV applications in standalone or in grid-connected mode [7]–[14].

The presence of an impedance network allows for the inclusion of inverter arm short-circuit states, which are prohibited in traditional inverters. This additional state is known as the "shoot-through" (ST) state, and it serves as a technique for increasing the input voltage[4], [15]. Accordingly, in this state, the inverter functions as a short-circuit by turning on at least two-phase leg switches concurrently.

In order to understand the operation of the QZSI and to efficiently design its control system, the authors, as in [8], [9], [11], [14], [16]–[18], use the small signal model of the impedance network and the inverter, where it is used to investigate the dynamic characteristics of the system and predict the influence of various parameters on the overall operation.

In the literature, several methods of controlling QZSI have been studied in order to stabilize the DC-link voltage [2], [19], as we know the DC-link voltage is an important element in the conversion process of the power from DC to AC as demonstrated in [5]. The DC-link voltage is mostly controlled by using proportional integral (PI) controller or by applying a non-linear control algorithm [19]. The linear control of QZSI, the command shoot-through duty ratio D is generated through the comparison of the input voltage V_{in}, the capacitor voltage V_C , or the Dc-link voltage V_{dc} to the corresponding reference value [2], [16], [19]. In the non-linear control, serval complex algorithms are invetagated, such as, slinding mode control [20], [21], predictive conrol model [22] and fuzzy logic control [23]. The non-linear control presents a fast dynamic response compared to PI controller [19]–[23]. Nonetheless, the complexity of these algorithms still prevents their application and encourages further research on linear control methods.

In the same way, this paper demonstrates the capability of QZSI to boost the input voltage in case of need. Also, the small signal model of QZSI is introduced to analyze and predict its dynamic characteristics. Then, these analyses will be used to design the controller in standalone mode. Similarly, a proposed two-loop linear control scheme, based on the SVPWM algorithm and PI controller, will be given and simulated on the Matlab/Simulink and Plecs software. Consequently, the simulation results illustrate the validity of the control scheme and controller addressed in this document.

The balance of this article is structured as follows: Section 2 includes the modeling of QZSI in steady state, the small signal model, the description of ZSVM algorithm and the proposed control scheme. In Section 3, the results of the dynamic characteristics analysis are firstly introduced, where the influence of various parameters is discussed. Then, the results of simulation of the proposed control scheme are presented and commented on. Finally, this paper will be concluded in Section 4 with a summary and the presentation of the perspectives of this work.

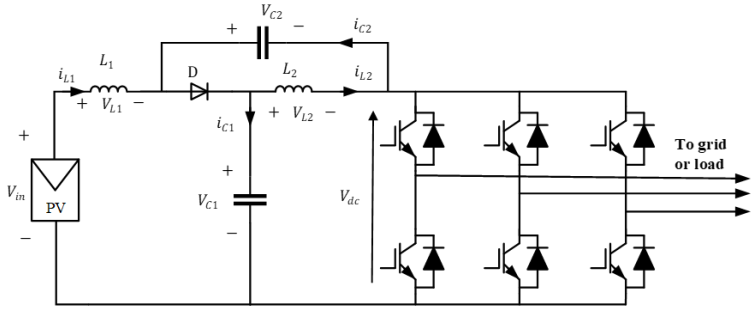

Figure 1. QZSI with continuous input current

2. PROPOSED RESEARCH METHOD

2.1. QZSI modeling

All Z-source inverter topologies have the same basic working principle, which necessarily includes the use of the switching shoot-throught state to the standard states.

To determine the dynamic model of QZSI we need to model the Quasi-Z-Source Network (QZSN) for each state, then the global model will be the average of models of each state [8], [16], [17], [24]. Figure 2 (a) and (b) show the equivalent circuit of QZSI for each state. For following, let $C = C_1 = C_2$and $L = L_1 = L_2$, the parasite resistances of inductors $r_L = r_{L1} = r_{L2}$ and series resistances of capacitors $r_C = r_{C1} = r_{C2}$.

During the NST state, the diode is forward-biased and will be in a conducting state. For simplification purposes, as outlined in [2], [16], the dynamic resistance and voltage drop associated with the diode will be disregarded.

For the rest, we take the following notations, T_c as the chopping cycle, T_S as the duration of the ST state and T_{NS} the duration of the NST state, with $T_C = T_s + T_{NS}$ and we specify $D = \frac{T_S}{T_C}$ as the duty ratio cycle.

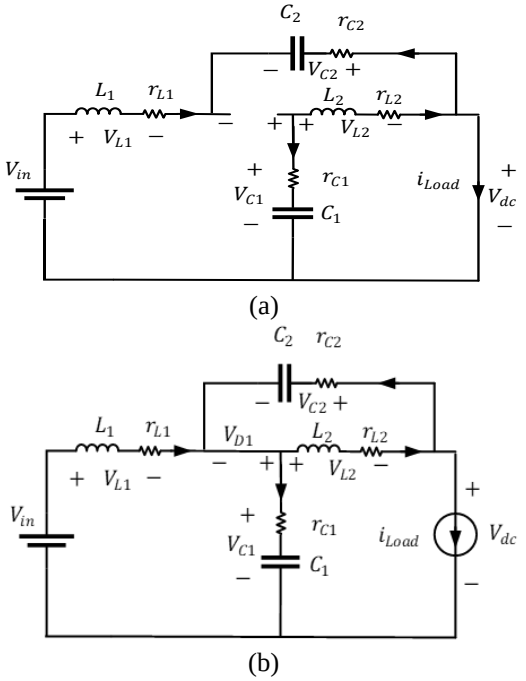

Figure 2. Equivalent circuit of QZSI(a): in Shoot-Through state (b): in Non-Shoot-Through state

2.1.1. Steady state model

All-previous research on ZSI family as in [8], [16], the chosen state vector for modeling QZSN is formed by the inductors current and capacitors voltage.

From Figure 1.a. during the ST state, we can write:

$$\dot{F}x = A_1 x + B_1 u = \begin{bmatrix} L & 0 & 0 & 0 \\ 0 & L & 0 & 0 \\ 0 & 0 & C & 0 \\ 0 & 0 & 0 & C \end{bmatrix} \begin{bmatrix} \dot{i}_{L1} \\ \dot{i}_{L2} \\ \dot{v}_{C1} \\ \dot{v}_{C2} \end{bmatrix} = \begin{bmatrix} -(r_L + r_C) & 0 & 0 & 1 \\ 0 & -(r_L + r_C) & 1 & 0 \\ 0 & -1 & 0 & 0 \\ -1 & 0 & 0 & C \end{bmatrix} \begin{bmatrix} i_{L1} \\ i_{L2} \\ v_{C1} \\ v_{C2} \end{bmatrix} + \begin{bmatrix} 1 & 0 \\ 0 & 0 \\ 0 & 0 \\ 0 & 0 \end{bmatrix} \bullet \begin{bmatrix} V_{in} \\ I_{Load} \end{bmatrix} \quad (1)$$

During the NST state, and from Figure 1. b., we can write:

$$\dot{F}x = A_2 x + B_2 u = \begin{bmatrix} L & 0 & 0 & 0 \\ 0 & L & 0 & 0 \\ 0 & 0 & C & 0 \\ 0 & 0 & 0 & C \end{bmatrix} \begin{bmatrix} \dot{i}_{L1} \\ \dot{i}_{L2} \\ \dot{v}_{C1} \\ \dot{v}_{C2} \end{bmatrix} = \begin{bmatrix} -(r_L + r_C) & 0 & 0 & 1 \\ 0 & -(r_L + r_C) & 1 & 0 \\ 0 & -1 & 0 & 0 \\ -1 & 0 & 0 & C \end{bmatrix} \begin{bmatrix} i_{L1} \\ i_{L2} \\ v_{C1} \\ v_{C2} \end{bmatrix} + \begin{bmatrix} 1 & r_C \\ 0 & r_C \\ 0 & -1 \\ 0 & -1 \end{bmatrix} \bullet \begin{bmatrix} V_{in} \\ I_{Load} \end{bmatrix} \quad (2)$$

We use the state space average method as described in [25] to deduce the DC side model of QZSI. We obtained the model described as below:

$$\dot{F}x = Ax + Bu \quad \text{where } A = DA_1 + (1-D)A_2 \quad \textit{and} \quad B = DB_1 + (1-D)B_2 \quad (3)$$

In the steady state, the previous model turn into $Ax + Bu = 0$, from this equation all steady state values of all voltages and currents can be deduced.

2.1.2. Small signal model

The steady state model, by its very nature, does not allow predicting the impact of a small disturbance on one of the input quantities [25]. Indeed, to design the control system of the inverter, it is necessary to know very well the dynamic behavior of the system. Furthermore, the non-linear time-varying nature of the switching

and PWM process renders the understanding and modeling of the system a highly challenging task, to overcome this limitation the state-space averaging method is used.

The relationship between the small signal state variables is deduced by introducing perturbations $\hat{d}, \hat{v}_{in}$ and $\hat{i}_{load}$ to d, v_{in} and i_{Load}. This perturbation induces a variation of $\hat{i}_{L1}, \hat{i}_{L2}, \hat{v}_{C1}$ and $\hat{v}_{C2}$ to the state variable i_{L1}, i_{L2} , v_{C1} and v_{C2}.

The averaged model that describes the dynamics of the QZSN is given by replacing $x = X + \hat{x}$ into equation (4). After developing the equations, the model is written as equation (4) shows [7]–[9], [13], [14], [16], [17]:

$$F\frac{d\hat{x}}{dt} = [A_1D + A_2(1-D)]\hat{x} + [B_1D + B_2(1-D)]\hat{u} + (A_1 - A_2)X\hat{d} + (B_1 - B_2)U\hat{d} = A\hat{x} + B\hat{u} + (A_1 - A_2)X\hat{d} + (B_1 - B_2)U\hat{d} \quad (4)$$

Thereafter, we need to deduce the transfer function of the system, for this purpose the elaborated small-signal model is transformed into a frequency-domain by applying the Laplace transformation to equation (4) and by using the flow graph method [2], the transfer functions small signal of the qZSN is described in Figure 3 .

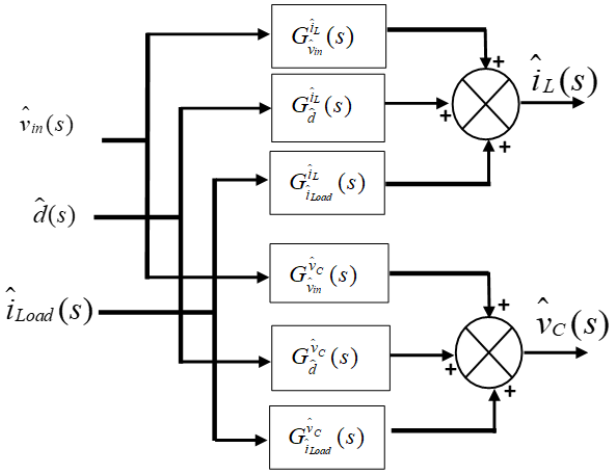

Figure 3.QZSI small signal model

All function transfer shown in Figure 3 is obtained by considering the other two inputs to be zero. As in [10], [16]–[18]. It can be stated that the transfer function from the duty ratio cycle $\hat{d}$ to the inductor currents $\hat{\imath}_{L1}$ and $\hat{\imath}_{L2}$ are identical, represented by $G_{\hat{d}}^{\hat{\imath}_L}(s)$ and the transfer function from duty ratio cycle $\hat{d}$ to the capacitor voltages $\hat{v}_{C1}$ and $\hat{v}_{C2}$ are also identical as $G_{\hat{d}}^{\hat{v}_C}(s)$. The most commonly used detailed transfer functions for designing a control system can be obtained as follows:

$$\begin{aligned}
G_{\hat{d}}^{\hat{v}_C}(s) &= \frac{I_0(Ls + r_L + r_C) + (1-2D)V_0}{LCs^2 + C(r_L + r_C)s + (1-2D)^2} \\
G_{\hat{d}}^{\hat{i}_L}(s) &= \frac{V_0Cs - (1-2D)I_0}{LCs^2 + C(r_L + r_C)s + (1-2D)^2} \\
G_{\hat{v}_{in}}^{\hat{v}_{C1}}(s) &= \frac{[LCs^2 + C(r_L + r_C)s + (1-2D)^2 + D^2]Cs}{[LCs^2 + C(r_L + r_C)s + (1-2D)^2][LCs^2 + C(r_L + r_C)s + 1]} \\
G_{\hat{i}_{Load}}^{\hat{i}_L}(s) &= \frac{(1-D)LCs^2 + (1-D)(r_L + r_C)Cs + (1-D)(1-2D)}{[LCs^2 + C(r_L + r_C)s + (1-2D)^2][LCs^2 + C(r_L + r_C)s + 1]}
\end{aligned} \quad (5)$$

2.2. SVPWM technique

The conventional PWM control techniques are not adapted for the ZSI/QZSI to meet their main objective. Indeed, several variants of PWM techniques adapted have been proposed in the literature. As, the simple boost[26], the maximum boost [27]and the maximum constant boost [28] that are the first methods proposed. Note that, these methods have been suggested to obtain a wider modulation range, a simpler

implementation, and a lower voltage stress on the switches. In this purpose, Due to its advantages of high DC voltage and low harmonics, the traditional space vector modulation (SVPWM) concept has been extended to ZSI/QZSI [6], [29], [30].

2.2.1. Traditional SVPWM

The SVPWM technique processes signals directly in the two-phase plane of the so-called Concordia transform(α−β), A control voltage vector is calculated globally and approximated, over a modulation period T_S, by an average voltage vector. The traditional SVPWM technique for the conventional VSI has eight voltage space states, including six active states and two zero states, and generates six sectors, I to VI as illustrated in Figure 4.

The algorithm to be implemented is well known as in [6], [29], [31],. The algorithm can be defined as follow:

$$Uref = \frac{T_1}{T_s}U_1 + \frac{T_2}{T_s}U_2 + \frac{T_0}{T_s}U_0 \quad where \begin{cases} T_1 = T_s M\, sin(\frac{\pi}{3}i - \theta) \\ T_2 = T_s M\, sin(\theta - \frac{\pi}{3}(i-1)) \end{cases} and \begin{cases} T_0 = T_s - T_1 - T_2 \\ M = \sqrt{3}\frac{U_{ref}}{V_{dc}} \end{cases} \quad (6)$$

By referring to the [29], [31], i denotes i^{th} sector (1 to 6), T_0 is the time interval of zero vector U_0; T_1 and T_2 are duration of active vectors U_1 and U_2, respectively, and θ is the angle between U_{ref} and U_1 as shown in Figure 4. M is the modulation index.

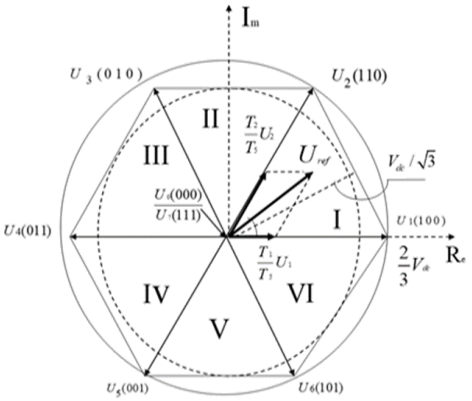

Figure 4. SVPWM sectors and vectors

Figure 5 presents the switching time sequence in the sector I, T_{min}, T_{mid} and T_{max} which defines the intervals of applications of each vector U_1, U_2 and U_0.

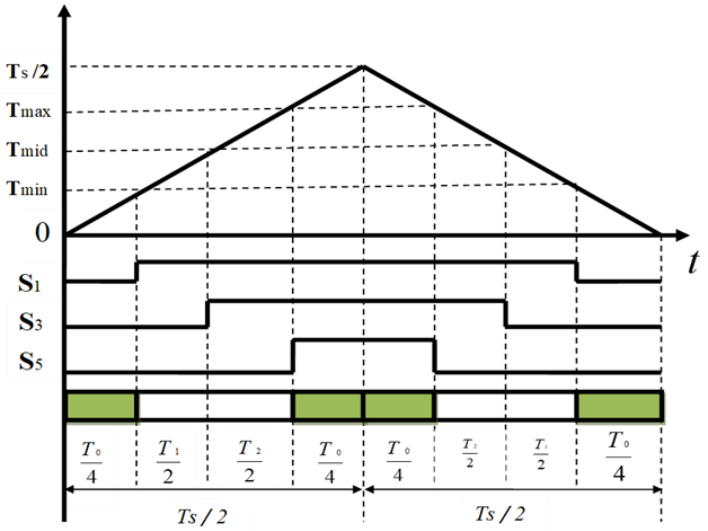

Figure 5. Switching time of SVM in sector I

2.2.2. Modified SVPWM

The modified SVPWM (called ZSVM) for ZSI/QZSI has the six active vectors, two zero vectors, and one extra ST vector as described in [29]. The reference output voltage will be written as:

$$Uref = \frac{T_1}{T_s}U_1 + \frac{T_2}{T_s}U_2 + \frac{T_0}{T_s}U_0 + \frac{T_{sh}}{T_s}U_{sh} \quad (7)$$

Where U_{sh} is the vector of the shoot-through state.

The ST state is inserted during the time intervals of the zero state, the active state is still unchanged. From the desired duty cycle ratio, the total time interval of the ST is deduced and equally divided into several parts per switching cycle, each part is inserted separately between the active state vector and the zero-state vector. Depending on the manner distributions of shoot-through part interval, there are three main types of SVMs for QZSI as described in [29], there are ZSVM6, ZSVM4 and ZSVM2. In this paper the ZSVM4 is used due to its advantages as presented in [29]. In the ZSVM4 the total ST time is divided in six parts, though it only modifies four switching control signals, The detailed switching patterns of ZSVM4 and more theoretical explanations can be found in [29].

2.3. Control scheme of QZSI

To boost and stabilize the DC-link voltage, various feedback control strategies of duty cycle ratio have been proposed [2], [7], [8], [16], [19], [32].For the off-grid application called also standalone mode, the control system is mainly formed by two stage control [19], [32], [33]. The first one consists on a Dc-link voltage control based on the shoot-through duty ratio, his main subject is to stabilize and maintain a DC-link peak voltage at the desired value V_{dc}^*. The second control stage is based on the ZSVM technique of the QZSI, this stage allows to improve output voltage and current profile and reduces the harmonics distortions.

Figure 6 shows the proposed QZSI control scheme. The desired DC-link voltage is compared to the DC-link voltage of the QZSI. The measurement of V_{dc} is very delicate because it is pulse voltage waveform due to ST state. To overcome this problem Vdc is estimated through the measurement of V_{C1}, the PI control is used to deduce the duty cycle ratio. The AC-side control in standalone mode is obvious, the synchronization block is not necessary. Indeed, the three output desired voltages are constructed and transformed in the $\alpha\beta$ plane. The switch control signals are delivered by programming the ZSVM4 algorithm described in section 4 and in [29].

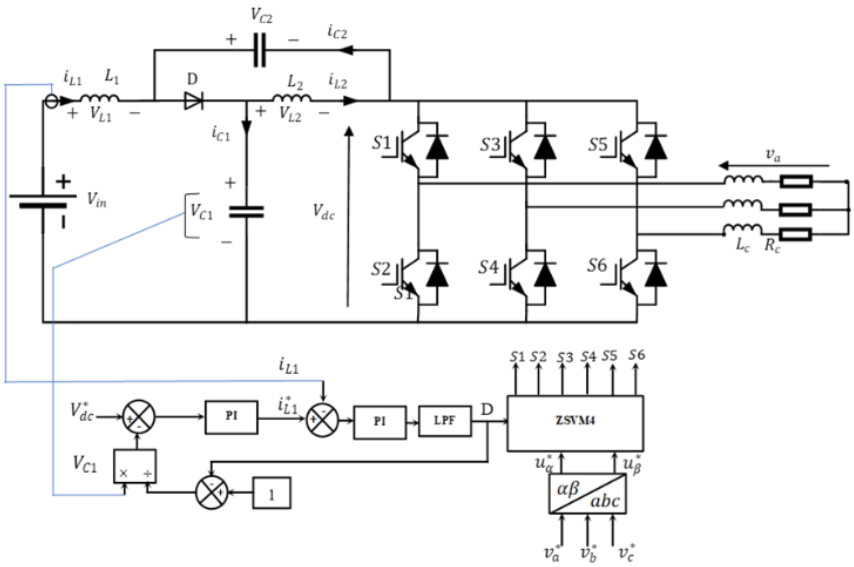

Figure 6. QZSI control system in standalone mode.

3. RESULTS AND DISCUSSION

3.1. Dynamic characteristics analysis

The elaborated model is very attractive for predicting the dynamic properties of the impedance network and inverter under varying parameters. taking into account the variation of the parameters of the

impedance network, i.e., L, C, r_L and r_C, as well as the variation of the duration of the shoot-through state, i.e., the duty cycle ratio D.

As mentioned, the transfer function from $\hat{d}$ to $\hat{v}_{C1}$ is the most significant in the controling system [2], [8], [16], [17], [32]. Table 1 presents the values of the various system parameters used to predict the dynamics characteristics of QZSN under parameters variations [9], [24].

Table 1. Parameters of the QZSI for dynamic characteristics analysis.

Parameters	Values	Parameters	values
L	500µH	Vin	130V
C	400µF	D	0.25
r_L	0.47 Ω	r_C	0.03 Ω
I_{load}	9.9A		

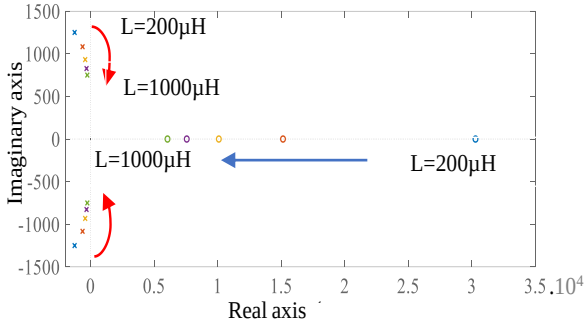

(a)

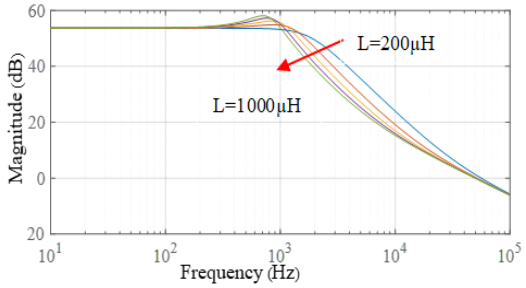

(b)

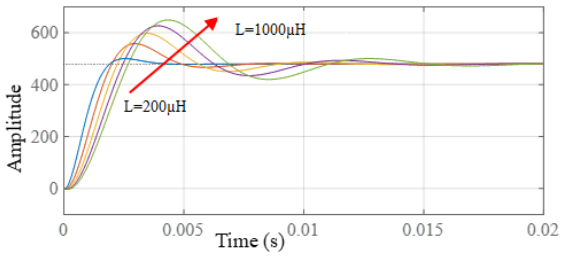

(c)

Figure 7. Characteristic dynamic analysis (a): Location of poles-zeros, (b): Bode diagram, (c): Step response, inductance variation

To being informed well about the dynamic's behavior of QZSN, different positions of the poles and zeros of $G_{\hat{d}}^{\hat{v}_C}(s)$ are studied by varying the parameter L. For the other parameters, the same studies are applied to predict their effects. The limited number of pages does not allow us to detail the influence of all the parameters.

Figure 7 shows the location of poles-zeros, bode diagrams and step responses of $G_{\hat{d}}^{\hat{v}_C}(s)$ with varying of the parameter L. The non-minimum phase (NMP) undershoot is marked by the existance of roots in right half-plane as Figure 7. (a) shows. As we seen in Figure 7 (b) when L increases, the settling time and the degree

of the NMP undershoot also increases. We can see also, from Figure 7 (c), that when L takes a small value, the of the step response presents a less overshoot, and also a small settling time . Thus,when L takes a large value, the steady state response took small ripples but the transient response got slow down.

The impact of other parameters,as duty ratio D, capacitor C and series resistance of the passive components impedance network, on the dynamic behavior of QZSI is determined in a similar way as in inductance variation.

3.2. Simulation results of standalone mode

To better test the proposed control system, two disturbances can be discussed, the variation of the input voltage (assimilated to a PV generator whose irradiance changes) or the variation of the load. Multiple numerical simulations under Plecs and Matlab/Simulink software were performed. In this paper, we will only present the results of the input voltage variation. Referencing to results of section 3, the capacitor and inductor of QZSI is chosen as provided by Table 1. The command value of peak DC-link voltage V_{dc}^{*} is set to 400V as in [34]. The simulated operation condition under input voltage changing is illustrated in Figure 8 :

- $0 \leq t \leq 0.7$, the input DC voltage $Vin = 260V$;
- $0.7 \leq t \leq 1.4$, the input DC voltage $Vin = 280V$;
- $t \geq 1.4$, the input DC voltage $Vin = 240V$;

The main results obtained are presented in Figure 9, Figure 10 and Figure 11.

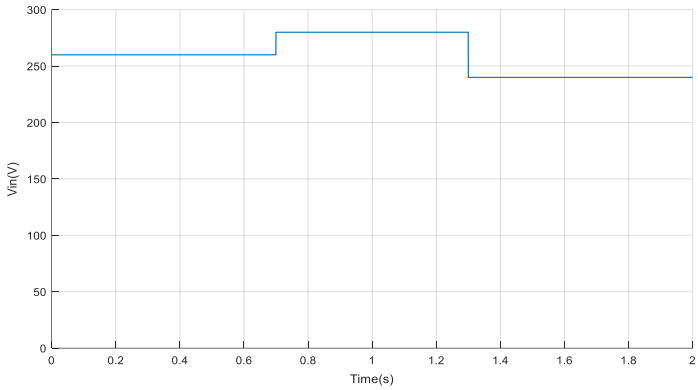

Figure 8. Input votage profil

3.2.1. DC link voltage

The main objective of the proposed control is to stabilize the DC link voltage because of its importance in the power conversion quality[5]. Figure 9 presents the DC-link voltage of QZSI supplied by the input voltage represented on Figure 8.

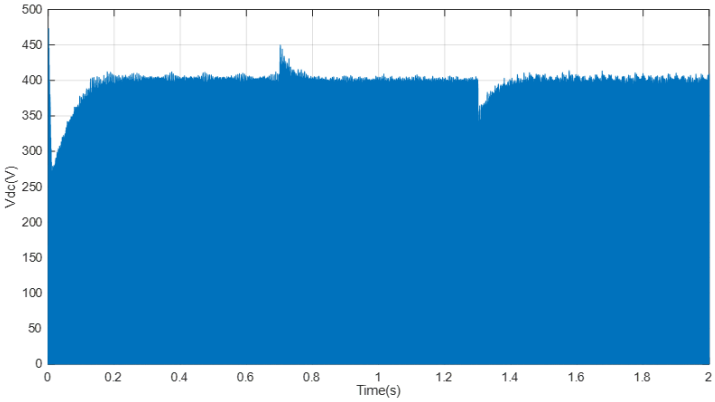

Figure 9. Regulated DC link voltage

As reported in [16], a change in the input voltage leads to persistent oscillations in the dc-link voltage, when the control loop is inappropriate. From Figure 9, it can be seen that the dc-link peak voltage is regulated and kept constant at the desired value (400V) regardless of the input voltage. Consequently, the proposed control scheme effectively eliminates oscillations in steady-state.

3.2.2. Duty Shoot-throught

From Figure 10 which present shoot-through duty ratio D, we can observe that when the input DC voltage increases or decreases, the duty cycle ratio D can decrease or increase respectively to obtain the desired DC-link voltage.

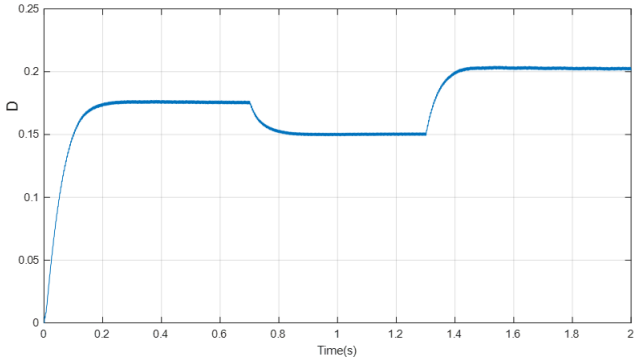

Figure 10. Shoot-through Duty ratio cycle

3.2.3. Output current

Figure 111 presents the output current profil, it could be mentionned that the output current stayed constant regardless of the input voltage because it depends only on the load.

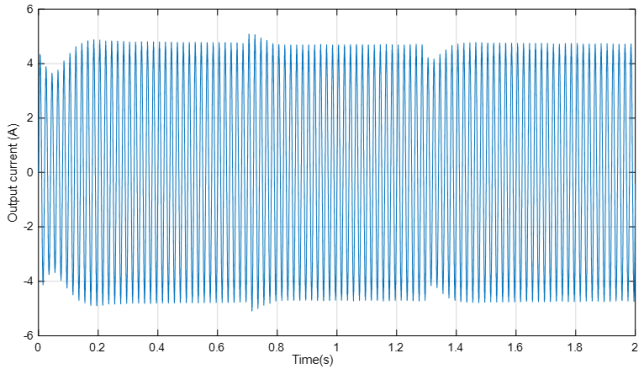

Figure 11. Output current

With the proposed control scheme, it can be concluded that the DC-link voltage is kept constant despite the variation of the input voltage, this is due to the regulation of the duty cycle by PI controllers.

4. CONCLUSION

This paper discusses the recently proposed QZSI converter which is widely used in photovoltaic power conversion. Due to its ability to increase the input voltage and harvest the maximum power. The detailed mathematical modeling of QZSI is occured. As to gain transfer functions we have used the state-space averaging method. Also, a comprehensive investigation of the dynamical features versus parameters variations of the QZSI network was carried out and reported, thereafter the techniques modulation adapted to ZSI/QZSI are discussed. Due to its advantages, the ZSVM4 is used in the scheme control proposed for QZSI in standalone mode. The simulations results confirm the validity of the scheme introduced whatever the nature of the disturbance. The next step is to propose a control scheme for grid-connected applications using MPPT algorithm for maximum power harvesting and applying a linear and non-linear control strategy.

REFERENCES

[1] S. Kouro, J. I. Leon, D. Vinnikov, and L. G. Franquelo, "Grid-connected photovoltaic systems: An overview of recent research and emerging PV converter technology," *IEEE Industrial Electronics Magazine*, vol. 9, no. 1, pp. 47–61, Mar. 2015, doi: 10.1109/MIE.2014.2376976.

[2] Y. Liu, H. Abu-Rub, B. Ge, F. Blaabjerg, O. Ellabban, and P. C. Loh, *Impedance source power electronic converters*. John Wiley & Sons, 2016.

[3] Y. P. Siwakoti, F. Z. Peng, F. Blaabjerg, P. C. Loh, and G. E. Town, "Impedance-source networks for electric power conversion part I: A topological review," *IEEE Trans Power Electron*, vol. 30, no. 2, pp. 699–716, 2014.

[4] F. Z. Peng, "Z-source inverter," *IEEE Trans Ind Appl*, vol. 39, no. 2, pp. 504–510, 2003.
[5] H. A. Ismail, A. Alenany, and B. Abozalam, "Improved dc-link voltage controller for photo voltaic on-grid systems," *Indonesian Journal of Electrical Engineering and Informatics*, vol. 9, no. 2, pp. 442–452, Jun. 2021, doi: 10.52549/ijeei.v9i2.1724.
[6] A. S. CS, V. Raghavendrarajan, R. H. Kumar, and M. Sasikumar, "An Interconnected Wind Driven SEIG System Using SVPWM Controlled TL Z-Source Inverter Strategy for Off-Shore WECS," *Indonesian Journal of Electrical Engineering and Informatics (IJEEI)*, vol. 1, no. 3, Sep. 2013, doi: 10.11591/ijeei.v1i3.89.
[7] Y. Li, F. Z. Peng, J. G. Cintron-Rivera, and S. Jiang, "Controller design for quasi-Z-source inverter in photovoltaic systems," in *2010 IEEE Energy Conversion Congress and Exposition*, 2010, pp. 3187–3194.
[8] A. O. AsSakka, M. A. ElShahed, M. A. M. Hassan, and T. Senjyu, "Modeling and control of a PV based QZSI for grid connected applications," in *2017 International Conference on Control, Automation and Information Sciences (ICCAIS)*, 2017, pp. 67–72.
[9] Y. Li, S. Jiang, J. G. Cintron-Rivera, and F. Z. Peng, "Modeling and control of quasi-Z-source inverter for distributed generation applications," *IEEE Transactions on Industrial Electronics*, vol. 60, no. 4, pp. 1532–1541, 2012.
[10] Z. Rasin, M. F. Rahman, M. Azri, M. H. N. Talib, and A. Jidin, "Design and Development of Grid-connected Quasi-Z-Source PV Inverter," *International Journal of Power Electronics and Drive Systems*, vol. 9, no. 4, p. 1989, 2018.
[11] L. Monjo, L. Sainz, J. J. Mesas, and J. Pedra, "Quasi-Z-Source Inverter-Based Photovoltaic Power System Modeling for Grid Stability Studies," *Energies (Basel)*, vol. 14, no. 2, 2021, doi: 10.3390/en14020508.
[12] T. Hou, C.-Y. Zhang, and H.-X. Niu, "Quasi-Z source inverter control of PV grid-connected based on fuzzy PCI," *Journal of Electronic Science and Technology*, vol. 19, no. 3, p. 100021, 2021, doi: https://doi.org/10.1016/j.jnlest.2020.100021.
[13] S. Jain, S. P. Nanduri, M. B. Shadmand, R. S. Balog, and H. Abu-Rub, "Direct decoupled active and reactive predictive power control of grid-tied quasi-Z-source inverter for photovoltaic applications," in *2017 IEEE Energy Conversion Congress and Exposition (ECCE)*, 2017, pp. 4582–4588. doi: 10.1109/ECCE.2017.8096784.
[14] W. Liu, Y. Yang, T. Kerekes, E. Liivik, and F. Blaabjerg, "Impedance Network Impact on the Controller Design of the QZSI for PV Applications," in *2020 IEEE 21st Workshop on Control and Modeling for Power Electronics (COMPEL)*, 2020, pp. 1–6. doi: 10.1109/COMPEL49091.2020.9265708.
[15] J. Anderson and F. Z. Peng, "Four quasi-Z-Source inverters," in *2008 IEEE Power Electronics Specialists Conference*, 2008, pp. 2743–2749. doi: 10.1109/PESC.2008.4592360.
[16] W. Liu, J. Yuan, Y. Yang, and T. Kerekes, "Modeling and control of single-phase quasi-Z-source inverters," in *IECON 2018-44th Annual Conference of the IEEE Industrial Electronics Society*, 2018, pp. 3737–3742.
[17] W. Liu, Y. Pan, and Y. Yang, "Small-Signal Modeling and Dynamic Analysis of the Quasi-Z-Source Converter," in *IECON 2019-45th Annual Conference of the IEEE Industrial Electronics Society*, 2019, vol. 1, pp. 5039–5044.
[18] T. Lannert, M. Isen, and M. Braun, "Small signal modeling of the quasi-Z-source-inverter and a novel control strategy to minimize the influence of input voltage disturbances," in *2013 15th European Conference on Power Electronics and Applications (EPE)*, 2013, pp. 1–10.
[19] Y. Liu, H. Abu-Rub, and B. Ge, "Z-source/quasi-Z-source inverters: Derived networks, modulations, controls, and emerging applications to photovoltaic conversion," *IEEE Industrial Electronics Magazine*, vol. 8, no. 4, pp. 32–44, 2014, doi: 10.1109/MIE.2014.2307898.
[20] F. Bagheri, H. Komurcugil, O. Kukrer, N. Guler, and S. Bayhan, "Multi-Input Multi-Output-Based Sliding-Mode Controller for Single-Phase Quasi-Z-Source Inverters," *IEEE Transactions on Industrial Electronics*, vol. 67, no. 8, pp. 6439–6449, Aug. 2020, doi: 10.1109/TIE.2019.2938494.
[21] A. Sangari, R. Umamaheswari, M. G Umamaheswari, and L. Sree B, "A novel SOSMC based SVPWM control of Z-source inverter for AC microgrid applications," *Microprocess Microsyst*, vol. 75, Jun. 2020, doi: 10.1016/j.micpro.2020.103045.
[22] D. Ma, K. Cheng, R. Wang, S. Lin, and X. Xie, "The Decoupled Active/Reactive Power Predictive Control of Quasi-Z-source Inverter for Distributed Generations," *Int J Control Autom Syst*, vol. 19, no. 2, pp. 810–822, 2021, doi: 10.1007/s12555-019-0698-9.
[23] T. Hou, C. Y. Zhang, and H. X. Niu, "Quasi-Z Source Inverter Control of PV Grid-Connected Based on Fuzzy PCI," *Journal of Electronic Science and Technology*, vol. 19, no. 3, pp. 274–286, 2021, doi: 10.1016/j.jnlest.2020.100021.
[24] E. Jaoide, F. el Aamri, M. Outazkrit, A. Radouane, and Az. Mouhsen, "Characteristics Dynamic Analysis and Modeling of Quasi-Z-Source Inverters for PV Applications," in *The Proceedings of the International Conference on Electrical Systems & Automation*, 2022, pp. 91–102.
[25] A. A. Elbaset and M. S. Hassan, "Small-Signal MATLAB/Simulink Model of DC–DC Buck Converter," in *Design and Power Quality Improvement of Photovoltaic Power System*, Springer, 2017, pp. 97–114.
[26] P. C. Loh, D. M. Vilathgamuwa, Y. sen Lai, G. T. Chua, and Y. Li, "Pulse-width modulation of Z-source inverters," in *Conference Record of the 2004 IEEE Industry Applications Conference, 2004. 39th IAS Annual Meeting.*, 2004, vol. 1, pp. 1–155. doi: 10.1109/IAS.2004.1348401.
[27] F. Z. Peng, M. Shen, and Z. Qian, "Maximum boost control of the Z-source inverter," *IEEE Trans Power Electron*, vol. 20, no. 4, pp. 833–838, 2005, doi: 10.1109/TPEL.2005.850927.
[28] M. Shen, J. Wang, A. Joseph, F. Z. Peng, L. M. Tolbert, and D. J. Adams, "Maximum constant boost control of the Z-source inverter," in *Conference Record of the 2004 IEEE Industry Applications Conference, 2004. 39th IAS Annual Meeting.*, 2004, vol. 1, pp. 1–147. doi: 10.1109/IAS.2004.1348400.
[29] Y. Liu, B. Ge, H. Abu-Rub, and F. Z. Peng, "Overview of Space Vector Modulations for Three-Phase Z-Source/Quasi-Z-Source Inverters," *IEEE Trans Power Electron*, vol. 29, no. 4, pp. 2098–2108, 2014, doi: 10.1109/TPEL.2013.2269539.

[30] A. Satif, L. Hlou, A. Zemmouri, H. Dahou, and R. Elgouri, "Real-time implementation of space vector modulation using arduino as a low-cost microcontroller for three-phase grid-connected inverter," *Indonesian Journal of Electrical Engineering and Informatics*, vol. 8, no. 1, pp. 10–20, Mar. 2020, doi: 10.11591/ijeei.v8i1.1207.
[31] A. Abdelhakim, F. Blaabjerg, and P. Mattavelli, "Modulation Schemes of the Three-Phase Impedance Source Inverters—Part I: Classification and Review," *IEEE Transactions on Industrial Electronics*, vol. 65, no. 8, pp. 6309–6320, 2018, doi: 10.1109/TIE.2018.2793255.
[32] Y. Liu, B. Ge, F. J. T. E. Ferreira, A. T. de Almeida, and H. Abu-Rub, "Modeling and SVPWM control of quasi-Z-source inverter," in *11th International Conference on Electrical Power Quality and Utilisation*, 2011, pp. 1–7.
[33] B. S. Eddine, K. Djallel, B. Noureddine, H. Ammar, and B. Abdelhak, "Quasi Z Source Inverter Output Voltage Regulation of Standalone System Powered by Photovoltaic Generators and Batteries," in *2017 International Renewable and Sustainable Energy Conference (IRSEC)*, 2017, pp. 1–6. doi: 10.1109/IRSEC.2017.8477284.
[34] Y. Liu, B. Ge, F. J. T. E. Ferreira, A. T. de Almeida, and H. Abu-Rub, "Modeling and SVPWM control of quasi-Z-source inverter," in *11th International Conference on Electrical Power Quality and Utilisation*, 2011, pp. 1–7. doi: 10.1109/EPQU.2011.6128914.

BIOGRAPHY OF AUTHORS

Essaid Jaoide was born in 27 January 1990 in Beni Mellal, Morocco. He is a PhD student in Laboratory of Radiation-Matter and Instrumenta- tion (RMI), Faculty of Sciences and Technology, Hassan 1st University, Morocco. he received his Master degree in electrical engineering from Cadi Ayyad University Marrakech, in 2013. He also obtained the Agrégation degree in Electrical Engineering in 2018. His researches are in fields impedance source power electronic converters and grid-connected photovoltaic systems. He can be contacted at email
e.jaoide@uhp.ac.ma

Faicel EL Aamri received his PhD on PV systems from Hassan first University in 2018. He currently works as Professor at Hassan II University, Faculty of Sciences and technologies of Mohammedia, Morocco. His area of research interest is the control of Grid-connected PV inverters and power electronics.

Mbarek Outazkrit received the M.S degree in electrical engineering from Cadi Ayyad University in 2014. He also obtained the Agregation degree in Electrical Engineering in 2016. Mbarek works in PhD at PhD Center of physics and engineering sciences in Hassan First University. His area of interest is modular multilevel converters MMC, power converter applications in power systems, grid integration of renewable energy sources.

Abdelhadi Radouane was born in 1969. He received the Agregation degree in Electrical Engineering from the ENSET of Rabat, Morocco in 1996. In 2017, he obtained a Ph.D in Automatic Control. Since 2018, he joined the FST Settat, Hassan First University of Settat, Morocco as Assistant-Professeur.

Azeddine Mouhsen Born in 10 July 1967, He is Professor of Physics at Hassan First University, Morocco, since 1996. He holds a PhD from Bordeaux I University (France) in 1995 and a thesis from Moulay Ismail University, Morocco, in 2001. He specializes in instrumentation and measurements, sensors, applied optics, energy transfer, radiation-matter interactions. He has taught courses in physical sensors, chemical sensors, instrumentation, systems technology, digital electronics and industrial data processing. He has published over 30 papers and he is the co-inventor of one patent. Actually, he is the Director of Laboratory of radiation-matter and Instrumentation. He can be contacted at email: az.mouhsen@gmail.com.